https://doi.org/10.20965/jdr.2016.p0246

Paper:

Real-Time Simulation of Dynamic Traffic Flow with Traffic Data Assimilation Approach

Yosuke Kawasaki, Yusuke Hara, Takuma Mitani, and Masao Kuwahara

Graduate School of Information Sciences, Tohoku University
6-6-06 Aramaki aza aoba, Aoba-ku, Sendai, Miyagi 980-8579, Japan
E-mail: kawasaki-y@plan.civil.tohoku.ac.jp
[Received September 29, 2015; accepted February 6, 2016]

The real-time traffic state estimation we propose uses a state-space model considering the variability of the fundamental diagram (FD) and sensing data. Serious congestion was caused by vehicle evacuation in many Sanriku coast cities following the great East Japan earthquake on March 11, 2011. Many of the vehicles in these congested queues were caught in the enormous tsunami after the earthquake [1]. Safe, efficient evacuation and rescue and restoration require that dynamic traffic states be monitored in real time especially in natural disasters. Variational theory (VT) based on kinematic wave theory is used for the system model, with probe vehicle and traffic detector data used to for measurement data. Our proposal agrees better with simulated benchmark traffic states than deterministic VT results do.

Keywords: traffic state estimation, data assimilation, kinematic wave theory, probe vehicle trajectory

1. Introduction

Natural disasters such as the great East Japan earthquake often cause serious traffic congestion and gridlock due to heavy evacuation by car. Hara and Kuwahara saw serious traffic jams in Ishinomaki city [1] that spread through the entire central urban area. This prevented large numbers of vehicles from moving and evacuating before the tsunami arrived, so many lives were lost. Avoiding such tragedies requires that traffic be monitored reliably in real time.

Against this background, we propose that monitors traffic states in real time based on a traffic flow model using all available sensing data. Because sensing data may not cover an entire study area, a traffic flow model is used to understand traffic states in areas that do not have sensing data. Our proposal uses both sensing data and a traffic flow model for assimilating data [2].

Among the many data assimilation models proposed, the variational theory (VT) proposed by Daganzo [3] is considered to be a data assimilation family because the VT cumulatively counts traffic based on a kinematic wave model and measurement data. The kinematic wave model has been authorized as a standard flow model that reasonably reproduces real phenomena [3]. The LWR model's key postulate is that a functional relationship exists between flow q and density k. This relationship, called the fundamental diagram (FD), may vary with location x but not with time t, as shown in **Fig. 1**. Given the FD and boundary condition, traffic states are usually estimated by using the kinematic wave model to solve the differential flow conservation equation along a characteristic curve on which flow is constant. The VT converts the problem to the shortest path calculation on a network specially designed based on the FD. Using two types of sensing data, i.e., probe vehicle and traffic detector data, Mehran et al. [4, 5] proposed a modified VT to deal with vehicles coming in and out of a study road section and to estimate trajectories of all vehicles running along a signalized arterial.

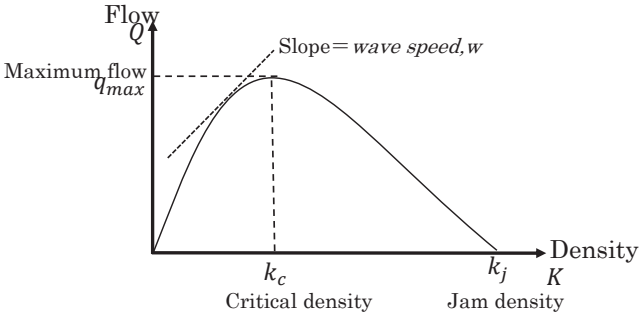

Fig. 1. Fundamental diagram.

Basically, the VT deterministically estimates traffic states, but several stochastic factors influence traffic state estimation. In free flow situation, for instance, the FD regulating driving behavior may vary among drivers who possess differing characters. In a disaster, the FD varies considerably due to exogenous factors such as many pedestrians and abandoned cars. Another stochastic factor lies in boundary traffic conditions, which are conventionally defined from sensing data. Mehran et al., for example, defined the boundary condition based on traffic counts of detectors installed at entrances and exits of the study section and on from probe vehicle trajectories. Traffic volume itself varies stochastically and contains random sensing errors. A probe trajectory may also have random measurement errors.

A promising data assimilation method for incorporating these stochastic properties into is the state-space model consisting of system and measurement models. Several recent studies reported using such a model include Chen et al.'s [6] state-space model for estimating travel time on motorways. Specifically, their model predicts travel time in a short time by matching the degree of similarity patterns between currently observed and previous travel time data. Dong et al. [7] proposed a state-space model estimating flow and speed on a motorway network. Claudel et al. [8] proposed data assimilation techniques for estimating motorway traffic states. A state-space model constructed based on the Hamilton-Jacobi equation uses GPS measurements. Deng et al. [9] proposed a similar data assimilation model using different data such as probe, bluetooth and traffic detector data. Yuan et al. [10] proposed using a Kalman filter using the LWR model for a system model with a traffic detector and probe data. Nates et al. [11] constructed a cell-based model similar to CTM for a local street and estimated traffic status by using an extended Kalman filter based on speed measurement from probe and bluetooth data. Patire et al. [12] and Vlahogianni et al. [13] summarized similar methods using probe and detector data.

The study covered in this paper is similary to the above literature in that an essentially kinematic wave model is used for the system model and probe and detector data are used for measurement. What makes this study unique, however, in FD and measurements is that the kinematic wave model is used for the system model with stochastic FD and that stochastic variability and random errors are considered in measurement.

2. State-Space Model Concept

2.1. Overview

The state-space model is a time-series model framework consisting of state and measurement vectors. The state vector consists of variables that cannot be observed, whereas the measurement vector consists of observational data. A system model represents the state vector time transition. The measurement model presents the relationship between state and measurement vectors. These models are developed as a conditional distribution and estimate the state vector that maximizes posterior distribution when the measurement vector is obtained time t. The relationship between the system and measurement models is shown in **Fig. 2**. Posterior distribution $p(\mathbf{x}_t|\mathbf{y}_t)$ is given in Eq. (1) based on the relationship shown in **Fig. 2** and the Bayes theorem:

$$p(\mathbf{x}_t|\mathbf{y}_t) \propto p(\mathbf{y}_t|\mathbf{x}_t)p(\mathbf{x}_t|\mathbf{y}_{1:t-1}) = p(\mathbf{y}_t|\mathbf{x}_t)\int p(\mathbf{x}_t|\mathbf{x}_{t-1})p(\mathbf{x}_{t-1}|\mathbf{y}_{1:t-1})d\mathbf{x}_{t-1} \quad \cdots (1)$$

$\mathbf{x}_t$ = state vector at time t

$\mathbf{y}_t$ = measurement vector at time t

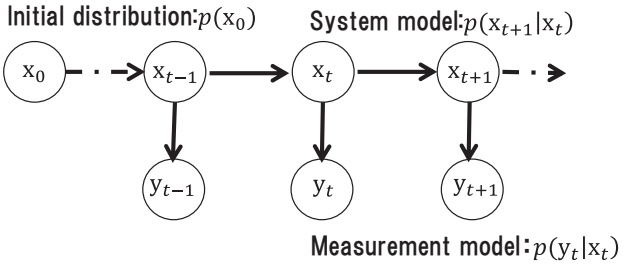

Fig. 2. Relationship between system and measurement models.

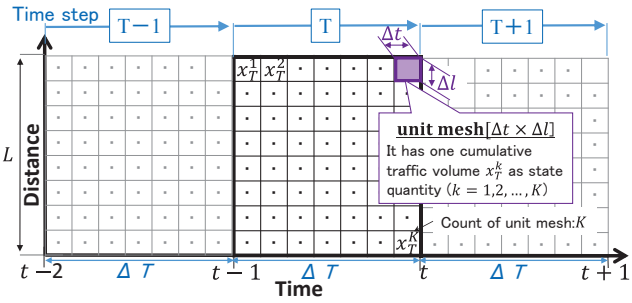

Fig. 3. Time-space mesh at time step T.

The state-space model must consider methods for calculating posterior distribution and for constructing measurement and system models.

2.2. State-Space Model Assumptions

The time axis is divided into small equal-length Δt intervals. Entire section length L is similarly divided into small equal-length Δl intervals. Area $(\Delta t \times \Delta l)$ is defined as a unit mesh. Together with integer number n, longer time unit ΔT is introduced with $\Delta T = n\Delta t$ and area $(\Delta T \times L)$ called time-space mesh T. The number of unit meshes in a time-space mesh is $nL/\Delta l\,(=K)$, as shown in **Fig. 3**. In our study, we use the loner time interval as the state space model time step.

The traffic state of the cumulative counts in unit mesh k in time-space mesh T is denoted as $x_T^{(k)}$, $k = 1,2,\ldots,K$. State vector $\mathbf{x}(T)$ is defined as a set of $x_T^{(k)}$:

$$\mathbf{x}(T) = \left(x_T^{(1)} \ldots x_T^{(k)} \ldots x_T^{(K)}\right)^t. \quad \cdots (2)$$

We define measurement vector $\mathbf{y}(T)$ in time-space mesh T. The observed value is also the cumulative traffic counts measured by a probe vehicle trajectory and upstream/downstream detectors. As shown in **Fig. 4**, a probe trajectory passing M_T unit meshes in time-space T yields M_T measurements and the measurement vector at the m-th unit mesh in time-space mesh T is written as

$$\mathbf{y}(T) = \left(y_T^{(1)} \ldots y_T^{(m)} \ldots y_T^{(M_T)}\right)^t, \quad m = 1,2,\ldots,M_T \le K. \quad \cdots (3)$$

We use a nonlinear system model and a linear measurement model:

$$\mathbf{x}(T) = f_{VT}(\mathbf{x}(T-1), \mathbf{v}_T), \quad \cdots (4)$$

$$\mathbf{y}(T) = \mathbf{H}_T\mathbf{x}(T) + \mathbf{w}_T, \quad \cdots (5)$$

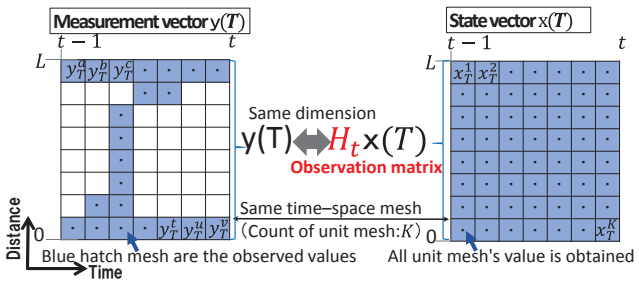

Fig. 4. Corresponding images of measurement and state vectors.

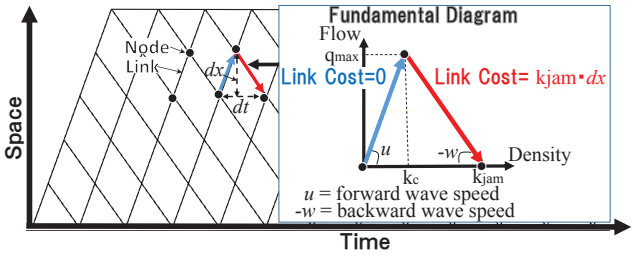

Fig. 5. FD network.

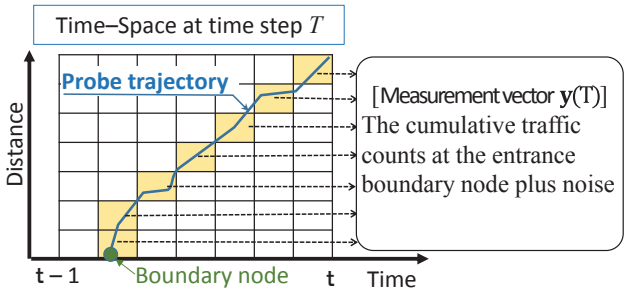

Fig. 6. Cumulative traffic volume in the observation image.

where $\mathbf{v}_T$ is system noise, $\mathbf{H}_T$ is assumed to be a unit matrix with dimension $(K \times M_T)$, and $\mathbf{w}_T$ is measurement noise. We use the VT, so a function of the system model $f_{VT}(\cdot)$ has suffix VT.

3. Construction of the State-Space Model

3.1. System Model

Given a piece-wise linear FD with forward wave speed u and backward wave speed $-w$, the FD network is constructed in two-dimensional time-space as shown in **Fig. 5**. The blue arrow shows a zero cost link with slope u associated with forward wave speed. The red link shows a link with slope $-w$ associated with backward wave speed. The cost of the red link is $k_{jam}dx = q_{max}dt$, in which dx and dt are space and time intervals as shown in **Fig. 5**. We define Ω_j: $\{i = 1, 2, \ldots, n_J\}$ as the set of reachable boundary node i to node j. N_i and N_j represent cumulative traffic counts at nodes i and j. Z_{ij} represents the amount of change in cumulative traffic counts between nodes i and j. Variational theory shows that cumulative counts at any interior node j are given by

$$N_j = \inf_i \left\{ N_i^B + Z_{ij} \right\}, \quad \Omega_j : \{i = 1, 2, \ldots, n_J\}. \quad . \quad (6)$$

where N_i^B is known cumulative counts at boundary node i. Z_{ij} is calculated by the shortest path cost from node i to j, provided that the FD is piece-wise linear. If Z_{ij} is calculated from all boundary nodes to node j, cumulative counts of node j are determined to have the lowest value.

Since our system model is a VT that determines cumulative counts at interior nodes given the cumulative counts at boundary nodes N_B and FD, $f_{VT}(\cdot)$ is written as

$$\mathbf{x}(T) = f_{VT}(\mathbf{x}(T-1), N_B(T), FD). \quad . \quad . \quad . \quad (7)$$

where $N_B(T)$ is cumulative counts at boundary nodes belonging to time-space mesh T. At initial time $T = 0$, $N_B(T)$ consists of cumulative counts measured by a traffic detector at the entrance and exit and probe trajectories available in time-space mesh T. The VT then determines all cumulative counts in a unit mesh in time-space mesh T, $\mathbf{x}(T)$, which in turn becomes the known boundary condition for the next time $T+1$. It calculates average cumulative traffic volume in a unit mesh when the FD network resolution is high enough.

The FD shape is determined by three parameters – q_{max}, K_c and K_{jam} – and the shape is assumed to vary stochastically due to the variabilities of q_{max} and K_c. The FD is then written as follows:

$$FD = f_{FD}(q_{\max} + \varepsilon, K_c + \gamma, K_{jam}). \quad . \quad . \quad . \quad . \quad (8)$$

where ε, γ are noises stochastically distributed. K_{jam} is assumed here to be a constant. Noise is assumed to follow uniform distributions.

3.2. Measurement Model

The measurement model requires (a–f) as follows:

a. Sensors for obtaining the observed values of the vehicle detector and GPS (probe)

b. Observation of cumulative traffic counts on the probe vehicle trajectory that travels through a one-scan interval of the system model

c. Use of probe vehicle trajectory data that flow from the upstream end of the target section only

d. Cumulative traffic counts of unit meshes where a probe vehicle passes in time-space mesh T stored in measurement vector $\mathbf{y}(T)$

e. No inflow or outflow traffic in the middle section, so cumulative traffic counts in unit meshes along the probe vehicle trajectory equal cumulative traffic counts at the entrance boundary node over which the probe vehicle passes as shown in **Fig. 6**

f. Measurement having errors as in Eq. (5) and error, i.e., the element of $\mathbf{w}_T$, assumed to follow an independent normal distribution with constant variance $N(0, \sigma_y^2)$

Table 1. Simulation conditions.

Length of section	1.0 km
Signal	4 units in the 200-m pitch
Simulation time	30 min
Volume (all vehicles)	300 cars
Volume (only probe car)	30 cars
Occurrence distribution of vehicle	Uniform distribution
S-V conditions*	Set different S-V* conditions for each vehicle
dt: Width of FD on FD network	1.0 s
Δt: Width of unit mesh	1.0 s
ΔT: Calculation time step in PFVT	300 s (= 5 min)

*S-V: Space clearance-Velocity

Based on the above assumptions and Eq. (5), the likelihood function is expressed as follows:

$$p(\mathbf{y}(T)|\mathbf{x}(T)) = \prod_{m=1}^{M_T} \frac{1}{\sqrt{2\pi\sigma_y^2}} \exp\left\{-\frac{1}{2\sigma_y^2}(y_t^{(m)} - (H_T\mathbf{x}(T))^{(m)})^2\right\}. \quad \cdots\cdots\cdots (9)$$

3.3. Particle Filter

Particle filtering [14] was used to calculate predicted and filtered states of all unit meshes. Given filtered state vector at time-space mesh $T\mathbf{x}(T-1)$ with its probability $p(\mathbf{x}(T-1)|\mathbf{y}(T-1))$ and measured boundary counts $N_B(T)$, the state vector $\mathbf{x}(T)$ is estimated based on the system model VT. A total of 1000 particles for this calculation are generated, which means that we repeat VT 1000 times. Based on the measurement model, measurement probability $p(\mathbf{y}(T)|\mathbf{x}(T))$ is calculated and the filtered state vector and probability $p(\mathbf{x}(T)|\mathbf{y}(T))$ are obtained from Eq. (1), thus forwarding time T.

4. Model Verification

4.1. Overview

Verification results of the proposed model are called a PFVT (particle filter based on the VT). The model is verified as detailed in the sections that follow.

4.1.1. Generation of Benchmark Data, FD and S-V Conditions

We create benchmark traffic state, i.e., trajectories of all vehicles, using traffic simulation. Traffic simulation conditions are shown in **Tables 1** and **2**. The simulated traffic state is shown in **Fig. 7**. Probe data are produced by extracting simulated vehicle trajectories randomly.

As shown in **Fig. 8**, the base FD is defined, then 300 FD patterns are made by generating ε and γ noise. ε and γ uniform distributions have ranges $\pm 20\%$ of q_{max} and K_c in the base FD. The 300 FD patterns are assigned to 300 generated vehicles in traffic simulation to create the benchmark traffic state.

The VT uses the base FD for calculation. Similarly 1000 FD patterns are made using the same uniform distributions for ε and γ for PFVT. To create 1000 different traffic states, the VT is used repeatedly 1000 times using each of the 1000 FD patterns.

Table 2. Signal cycle (s) conditions.

	Blue	Yellow	Red	Cycle	Offset
Signal 1	117	3	30	150	0
Signal 2	117	3	30	150	5
Signal 3	117	3	30	150	10
Signal 4	57	3	30	90	15

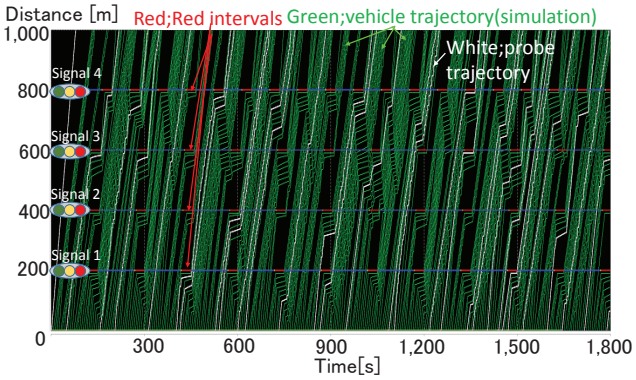

Fig. 7. Benchmark data, i.e., trajectory data for all vehicles.

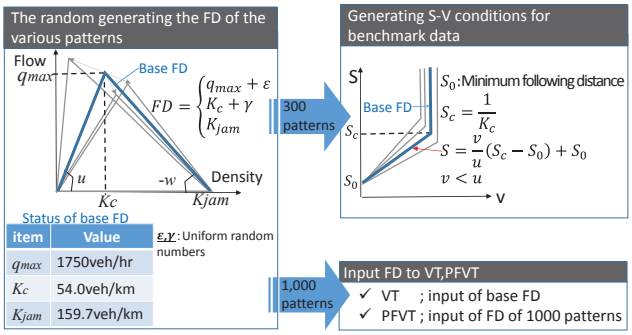

Fig. 8. Generation of FD and S-V conditions.

4.1.2. Traffic State Estimation and Accuracy Verification

Temporal and spatial cumulative traffic volumes are estimated with the VT and PFVT using probe data, both upstream and downstream volumes, and signal data as input. Calculation time step ΔT of PFVT is 300 seconds. The model's accuracy is verified by comparing the traffic volumes and traffic congestion situations obtained using the VT and PFVT with each other and with corresponding values in benchmark data. We last analyze the relationship between the probe data-extraction rate and the cumulative traffic volume with estimated accuracy. Because

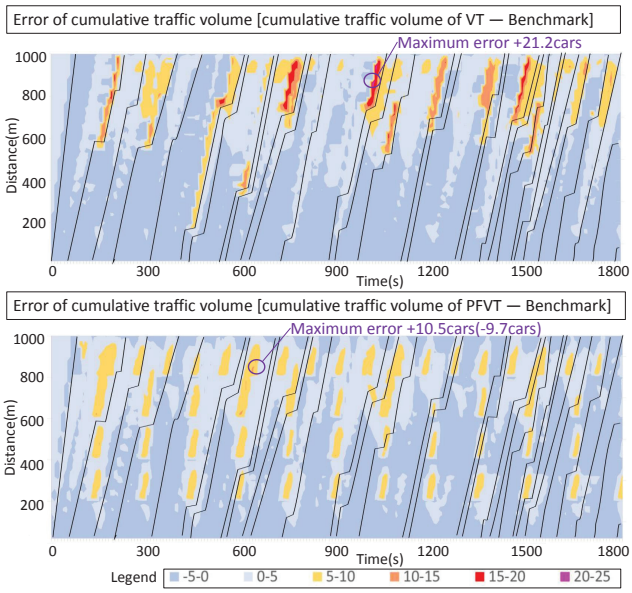

Fig. 9. Estimation error heat map in cumulative traffic volume.

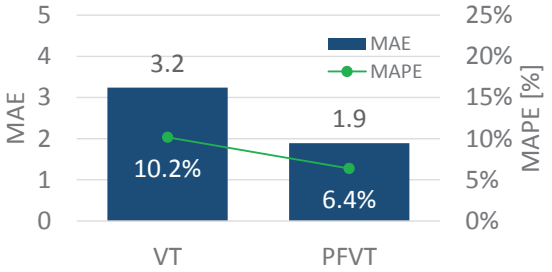

Fig. 10. Comparison of estimation errors MAE and MAPE.

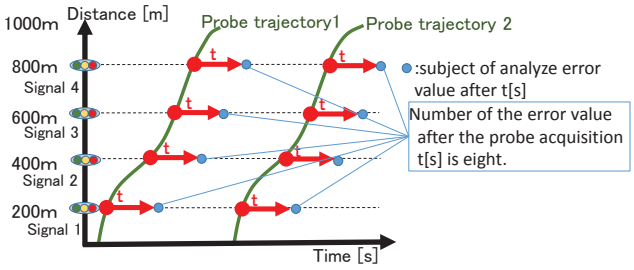

Fig. 11. Subject of the error value after probe acquisition in time-space.

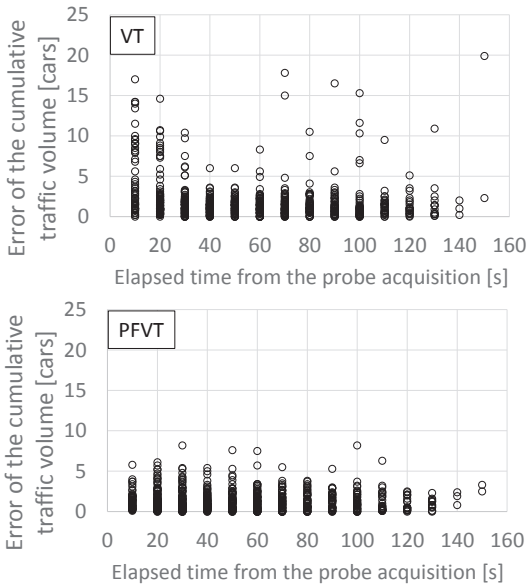

Fig. 12. Relationship between elapsed time and the error in the cumulative traffic volume from probe acquisition.

spatiotemporal nodes have different positions in the VT and PFVT, we count the cumulative traffic volume with an average mesh value of 10 s × 20 m.

4.2. Cumulative Traffic Volume Verification

The estimation error of the cumulative traffic volume is evaluated using the mean absolute error (MAE), mean absolute percentage error (MAPE), and an estimation error heat map. Statistically, MAE and MAPE are used to measure how closely forecasts or predictions compare to eventual outcomes. MAE and MAPE are defined as follows:

$$\mathrm{MAE} = \frac{1}{n}\sum_{k=1}^{n}|x_k - \hat{x}_k|, \quad \ldots\ldots\ldots\ldots (10)$$

$$\mathrm{MAPE} = \frac{100}{n}\sum_{k=1}^{n}\left|\frac{x_k - \hat{x}_k}{x_k}\right|. \quad \ldots\ldots\ldots\ldots (11)$$

n is the number of elements in the dataset, x_k is the true cumulative traffic volume (here, these are simulation results), and subscript k indicates the index of x. $\hat{x}_k$ is an estimate of the cumulative traffic volume based on the model. **Fig. 9** shows an estimation error heat map. The estimation error magnitude of the cumulative traffic volume in time-space is expressed by a color. Error with the PFVT is smaller than that with the VT. The maximum error with the VT is 21.2 cars, whereas that with the PFVT is 10.5 cars, i.e., −9.7 cars. In addition, with PFVT, errors around the probe trajectory and upstream section are relatively small. Average errors in cumulative traffic volume estimation are compared in **Fig. 10**. The PFVT MAE is 1.9 and that of PVFT MAPE is 6.9%, while those of the VT are 3.2 and 10.2%. MAE and MAPE values obtained with the PFVT are approximately 40% smaller than those obtained with the VT. To grasp the relationship between cumulative traffic volume error and the probe data trajectory, we analyzed the elapsed time relationship from error distribution in time-space and probe acquisition, defining the error value analysis subject after probe acquisition as shown in **Fig. 11**. We created signal installation site error. In the following case of **Fig. 11**, the number of the error value after probe acquisition t [s] is eight. The relationship between elapsed time and cumulative traffic volume error from probe acquisition is shown in **Fig. 12**. The error value of the VT is greater than that of the PFVT. VT error values are more varied than those of the PFVT. Bubble charts show the error value for each distance in **Fig. 13**. VT error increases with the distance from the starting point. Maximum VT error occurs at the point most distant from the start, with a distance of 800 m and

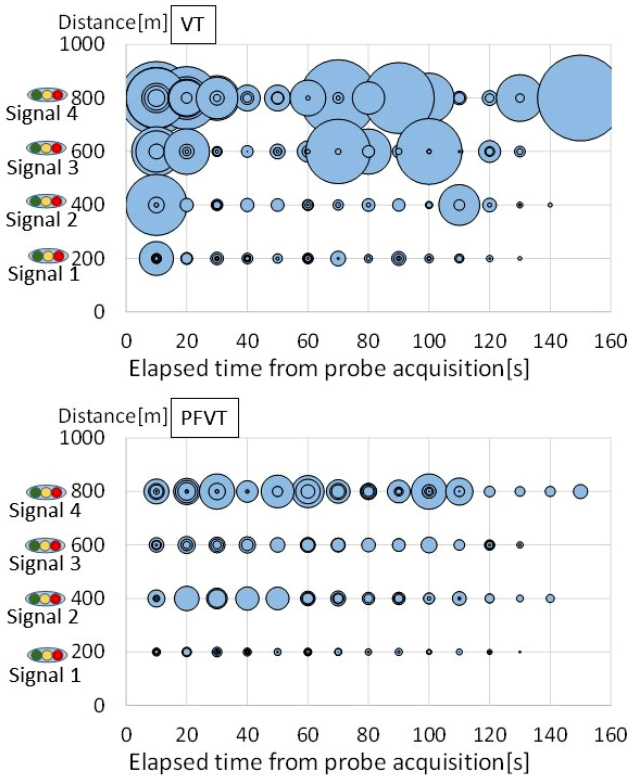

*Radius of the circle indicates the magnitude of the error.

Fig. 13. Relationship between elapsed time from probe acquisition and error distribution for each cross-section.

an elapsed time from probe acquisition of 150 s. PFVT error is smaller than that of the VT.

4.3. Traffic Congestion State Verification

The traffic congestion state is diagrammed as shown in **Fig. 14**. In benchmark data (true values), signals 3 and 4 represent a bottleneck, i.e., the beginning of traffic congestion). In the VT model, the downstream section of signal 4 is thought to be a bottleneck, but this does not correspond to a bottleneck in benchmark data. In contrast, the PFVT estimate suggests a bottleneck (signals 3 and 4) similar to that of benchmark data. The congestion-length estimate is relatively accurate.

To determine the accuracy of estimated speed, we compared concordance ratios of the speed level. We first divided the estimated speed of each mesh into 40 km/h or more, 30–40 km/h, 20–30 km/h, and 0–20 km. We then compared matching ratios of speed level in the same mesh (10 s × 20 m) in the time-space between benchmark data and the model. The speed level concordance ratio is as follows:

$$P_c = \frac{n_c}{N} \times 100. \quad \ldots\ldots\ldots\ldots (12)$$

P_c is the concordance ratio (%), N is the total number of meshes in time space, and n_c is the mesh number of the speed level to be matched. As shown in **Fig. 15**, the speed level concordance rate is 38% in the VT and 50% in the PFVT, so the PFVT is higher than the VT. Because the

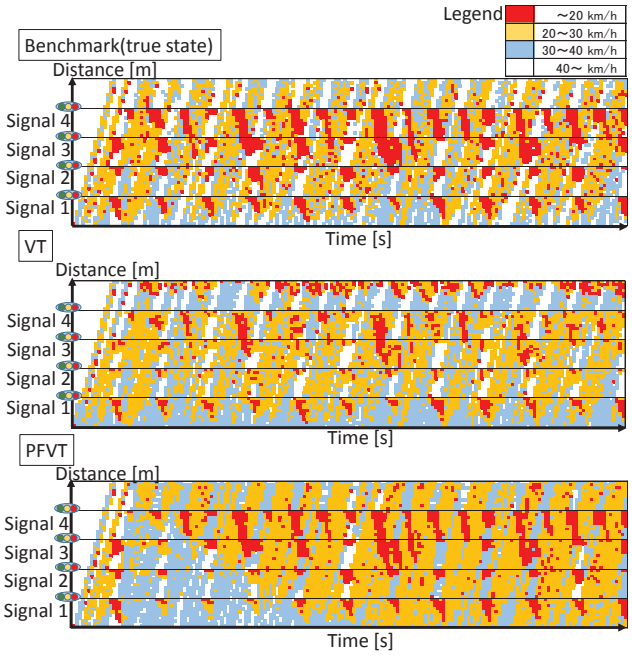

Fig. 14. Traffic congestion state diagram.

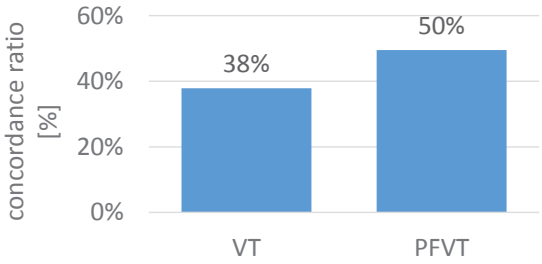

Fig. 15. Speed level concordance ratio.

VT model estimates that no congestion exists at the true bottleneck position, we concluded that the concordance rate of the VT is lower than that of the PFVT.

To describe precision, recall, and F-measure analysis results. Precision and recall are used as evaluation indicators of information retrieval validity. Precision is the percentage of correct data in search results (estimated results by model). Recall is the percentage of search results in all correct data. The F-measure is the harmonic mean value of precision and recall, which generally have a trade-off relationship. A higher F-measure means that the model performs better [15]. We define precision and recall in this study. We first define congestion as speeds of less than 20 km/h, then define the relationship between actual traffic conditions (correct data) and the estimated traffic state by the model, as shown in **Table 3**. Precision, recall, and F-measure equations are as follows:

$$Precision = \frac{TP}{TP+FP}; \quad \ldots\ldots\ldots\ldots (13)$$

$$Recall = \frac{TP}{TP+FN}; \quad \ldots\ldots\ldots\ldots (14)$$

$$F\text{-}measure = \frac{2 \times Precision \times Recall}{Precision + Recall}. \quad \ldots\ldots (15)$$

Table 3. Relationship between the model's true and estimated traffic states.

		True traffic state	
		Congestion	Non-congestion
Model	Congestion	TP (True Positive)	FP (False Positive)
	Non-congestion	FN (False Negative)	TN (True Negative)

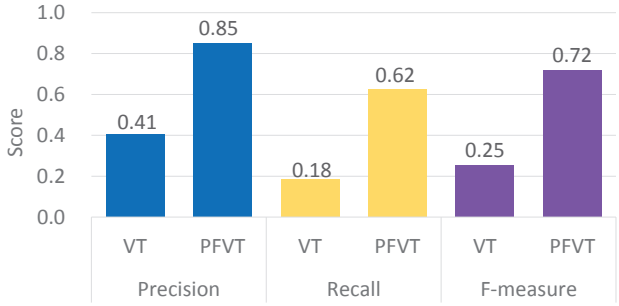

Fig. 16. Precision, recall, and F-measure.

TP, *FP*, and *FN* are the number of meshes on the time-space that corresponds to the relationship in **Table 3**. From the equation, this is at $0 \leqq F\text{-}measure \leqq 1$ because it is $0 \leqq Precision \leqq 1$ and $0 \leqq Recall \leqq 1$. Precision, recall, and f-measure are shown in **Fig. 16**. Precision is 0.41 in the VT model and 0.85 in the PFVT model. Recall is 0.18 in the VT and 0.68 in the PFVT and F-measure is 0.25 in the VT and 0.72 in the PFVT.

4.4. Relationship Between the Probe Vehicle Ratio and Accuracy

MAE of the cumulative traffic volume is calculated for probe vehicle ratios from 10% to 50% and the accuracy between models is compared. The relationship between the probe vehicle ratio and MAE is shown in **Fig. 17**. When the probe vehicle ratio increases, MAE values of the VT and PFVT models are in close proximity, but when the probe vehicle ratio is 50%, there is almost no difference in MAE between the VT and PFVT. Even if the probe ratio becomes high, the MAE value of the PFVT model does not decrease as that of the VT model does.

4.5. Model Verification Results

In Section 4.2, we verified estimated cumulative traffic count results. MAE and MAPE values obtained with the PFVT are approximately 40% smaller than those obtained with the VT, and VT error increases with the distance from the entrance boundary. Maximum VT error is found in a location 800 m downstream from the entrance in 150 seconds of time elapsed from probe data acquisition.

In Section 4.3, we verified estimated results in a congested situation. Although the downstream end of signal 4

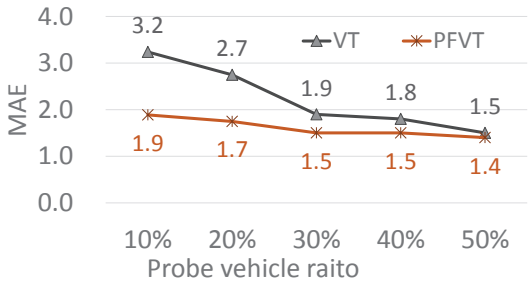

Fig. 17. Relationship between the probe vehicle ratio and MAE.

is a bottleneck in the VT, this location is not a bottleneck in benchmark data. In contrast, the PFVT finds the bottleneck at the same location as in benchmark data. The PTVT has a statistically more reasonable result because of the higher F-value of 0.72 than that of the VT at 0.25. The FD changes continuously in benchmark data, but the VT used one FD. Error caused by the time-varying FD expands with time. The PFVT is the traffic state estimated by selecting a highly likely FD. The PTVT thus follows FD change and shows relatively high accuracy.

In Section 4.4, MAE of cumulative traffic counts are calculated for different percentages of probe vehicles. As the percentage of probe vehicles increases, MAE values of the VT and PFVT become closer, that is, VT and PTVT MAEs become almost the same with 50% probe inclusion. In this example, the VT estimated the traffic state with good accuracy with such a high percentage of probe vehicles. Especially in a disaster, however, such a high percentage of probe vehicles may not be expected and the PTVT seems more reliable with lower probe inclusion.

5. Conclusions

This study uses a state space model to assimilate the VT with observed probe data to account for FD variability. FD variability is considered by the stochastically fluctuated shapes of FDs and the probabilities of traffic states are estimated by using a particle filter. Model verification using benchmark data shows that the proposed model agrees better with the benchmark traffic state compared to the VT. In principle, the proposed PTVT considers stochastic variations of the FD as well as boundary conditions, so it must show better results than a VT that deterministically estimates traffic states. Although VT results are brought closer to 1 by the PTVT as the percentage of probe vehicles increases, the PTVT appears more promising under the current situation with a lower penetration rate, especially in a natural disaster.

We list the following future challenges:

1) Construction of advanced models
   In this study, we assumed no inflow or outflow traffic in the middle section and constructed a model accordingly. Traffic does exist that flows in and out of an intersection in the middle, however, so a system model must be constructed to consider this effect

of inflow and outflow traffic. An observation model must also be constructed to evaluate the probe vehicle that traverses the middle section.

2) Application of the model to different regions
Model performance must be confirmed by applying the proposal to different regions. New challenges must also be extracted.

3) Traffic state estimation by data fusion
One way to estimate the traffic situation during disasters is to fuse datasets. It is possible to gain much information, for example, by fusing images of affected areas, Twitter data (text data from tweets), and weather information. This offers a multifaceted understanding of the situation and the possibility of obtaining more reliable information.

Acknowledgements

This research was supported by "Establishing the most advanced disaster-reduction management system by fusion of real-time disaster simulation and big data assimilation," Japan Science and Technology Agency (JST, CREST).

References:

[1] Y. Hara and M. Kuwahara, "Traffic Monitoring immediately after a major natural disaster as revealed by probe data – A case in Ishinomaki after the Great East Japan Earthquake," Transportation Research Part A: Policy and Practice, Vol.75, pp. 1–15, 2015.
[2] M. L. John, S. Lakshmivarahan, and S. K. Dhall, "Dynamic Data Assimilation: A Least Squares Approach," CAMBRIDGE, 2006.
[3] C.F. Daganzo, "On the Variational Theory of Traffic Flow: well-posedness, duality and applications," Networks and Heterogeneous Media, Vol.1, No.4, pp. 601–619, 2006.
[4] B. Mehran, M. Kuwahara, and F. Naznin, "Implementing kinematic wave theory to reconstruct vehicle trajectories from fixed and probe sensor data," Transportation Research Part C: Emerging Technologies, Vol.20, No.1, pp. 144–163, 2012.
[5] B. Mehran and M. Kuwahara, "Fusion of probe and fixed sensor data for short-term traffic prediction in urban signalized arterials," Int. Journal of Urban Sciences, Vol.17, No.2, pp. 163–183, 2013.
[6] H. Chen and H.A. Rakha, "Real-time travel time prediction using particle filtering with a non-explicit state-transition model," Transportation Research Part C: Emerging Technologies, Vol.43, No.1, pp. 112–126, 2014.
[7] C. Dong, C. Shao, S.H. Richards, and L.D. Han, "Flow rate and time mean speed predictions for the urban freeway network using state space model," Transportation Research Part C: Emerging Technologies, Vol.43, No.1, pp. 20–32, 2014.
[8] C.G. Claudel and A.M. Bayen, "Convex Formulations of Data Assimilation Problems for a Class of Hamilton-Jacobi Equations," SIAM Journal on Control and Optimization, Vol.49, No.2, pp. 383–402, 2011.
[9] W. Deng, H. Lei, and X. Zhou, "Traffic state estimation and uncertainty quantification based on heterogeneous data sources: A three detector approach," Transportation Research Part B: Methodological, Vol.57, pp. 132–157, 2013.
[10] Y. Yuan, A. Duret, and H. van Lint, "Mesoscopic Traffic State Estimation based on a Variational Formulation of the LWR Model in Lagrangian-space Coordinates and Kalman Filter," Transportation Research Procedia, Vol.10, pp. 82–92, 2015.
[11] A. Nantes, D. Ngoduy, A. Bhaskar, M. Miska, and E. Chung, "Real-time traffic state estimation in urban corridors from heterogeneous data," Transportation Research Part C: Emerging Technologies, Vol.61, 2015.
[12] A.D. Patire, M. Wright, B. Prodhomme, and A. M. Bayen, "How much GPS data do we need?," Transportation Research Part C: Emerging Technologies, Vol.58, pp. 325–342, 2015.
[13] E.I. Vlahogianni, M.G. Karlaftis, and J.C. Golias, "Short-term traffic forecasting: Where we are and where we're going," Transportation Research Part C: Emerging Technologies, Vol.43, No.1, pp. 3–19, 2014.
[14] G. Kitagawa, "Monte Carlo Filter and Smoother for Non-Gaussian Nonlinear State Space Models," Journal of Computational and Graphical Statistics, Vol.5, No.1, pp. 1–25, 1996.
[15] J. Han, M. Kamber, and J. Pei, "DATA MINING Concepts and Techniques Third Edition," The Morgan Kaufmann Series in Data Management Systems, 2011.

Name:
Yosuke Kawasaki

Affiliation:
Researcher, Graduate School of Information Sciences, Tohoku University

Address:
6-6-06 Aramaki aza aoba, Aoba-ku, Sendai, Miyagi 980-8579, Japan

Brief Career:
2005- Civil Engineer, Oriental Consultants Co., Ltd.
2014- Reserecher, Tohoku University

Selected Publications:
• Y. Kawasaki, A. Tanaka, H. Goto, T. Takada, H. Warita, S. Hong, S. Tanaka, and M. Kuwahara, "Research on Mechanisms to Provide Attention-attracting Information Effective in Preventing Rear-end Collisions," ITS World Congress, Orlando, 2011.

Academic Societies & Scientific Organizations:
• Japan Society of Civil Engineers (JSCE)
• Japan Society of Traffic Engineers (JSTE)
• Information Processing Society of Japan (IPSJ)

Name:
Yusuke Hara

Affiliation:
Researcher, Graduate School of Information Sciences, Tohoku University

Address:
6-6-06 Aramaki aza aoba, Aoba-ku, Sendai, Miyagi 980-8579, Japan

Brief Career:
2011- Research Fellow of the Japan Society for the Promotion of Science (JSPS)
2012- Assistant Professor, Tohoku University
2015- Researcher Precursory Research for Embryonic Science and Technology (PREST) (concurrent)

Selected Publications:
• Y. Hara and M. Kuwahara, "Traffic Monitoring immediately after a Major Natural Disaster as Revealed by Probe Data – a Case in Ishinomaki after the Great East Japan Earthquake," Transportation Research Part A: Policy and Practice, Vol.75, pp. 1-15, 2015.

Academic Societies & Scientific Organizations:
• Japan Society of Civil Engineers (JSCE)
• Japan Society of Traffic Engineers (JSTE)
• City Planning Institute of Japan (CPIJ)

Name:
Takuma Mitani

Affiliation:
Researcher, Graduate School of Information Sciences, Tohoku University

Address:
6-6-06 Aramaki aza aoba, Aoba-ku, Sendai, Miyagi 980-8579, Japan

Brief Career:
2006- Civil Engineer, Fukken Co., Ltd.
2013- Assistant Professor, Tohoku University

Selected Publications:
• E. Hato, S. Itsubo, and T. Mitani, "Development of MoALs (mobile activity loggers supported by gps-phones) for Travel Behavior Analysis," TRB Annual Meeting in Washington DC, 2006.

Academic Societies & Scientific Organizations:
• Japan Society of Civil Engineers (JSCE)
• Japan Society of Traffic Engineers (JSTE)
• City Planning Institute of Japan (CPIJ)
• Information Processing Society of Japan (IPSJ)

Name:
Masao Kuwahara

Affiliation:
Researcher, Graduate School of Information Sciences, Tohoku University

Address:
6-6-06 Aramaki aza aoba, Aoba-ku, Sendai, Miyagi 980-8579, Japan

Brief Career:
1985- Joined University of Tokyo
1987- Associate Professor, University of Tokyo
2000- Professor, University of Tokyo
2010- Professor, Tohoku University

Selected Publications:
• B. Mehran, M. Kuwahara, and F. Naznin, "Implementing kinematic wave theory to reconstruct vehicle trajectories from fixed and probe sensor data," Transportation Research Part C 20, pp. 144-163, 2012.

Academic Societies & Scientific Organizations:
• Japan Society of Civil Engineers (JSCE)
• Japan Society of Traffic Engineers (JSTE)
• International Association on Transportation and Traffic Safety (IATSS)